Measurement Settings' Influence upon Energy Detection of TETRA Signals

Radu MITRAN, Paul BECHET
Nicolae Balcescu Land Forces Academy of Sibiu
str. Revolutiei 3-5, RO-550170 Sibiu
radumitran@yahoo.com, pbechet@gmail.com

***Abstract*—The present paper aims to determine the optimum parameters for the detection of downlink TETRA signals, through energy measurement. In order to optimize the detection parameters we have assessed the probabilities of detection and of false alarm, based on the estimated power distributions, measured by the Parzen method. The TETRA signals power has been measured with an experimental system, the data having been processed by MATLAB software. The obtained results could contribute to the improvement of TETRA mobile station algorithms with the aim of base stations broadcasting channels detection and to the improvement of the measurement system settings in order to obtain the coverage maps of the TETRA base stations.**

***Index Terms*—energy detector, spectrum analyzer, TETRA**

I. INTRODUCTION

The Terrestrial Trunked Radio standard (TETRA), defined by European Telecommunications Standards Institute (ETSI) as a standard for private mobile communications [1], was specifically designed for use by government agencies. TETRA offers services of voice communication and data transmission at low bit rates (<12 kbps). In order to achieve higher rates, a new TETRA 1-compliant standard (TEDS - TETRA Enhanced Data Service*)* has been developed [2]. It supports high-speed data transmission at a maximum speed of 518 kbps. This increase in transmission speed entailed changes in the RF channel bandwidth and modulation schemes.

The changes that TEDS brings to the radio interface are significant as compared to TETRA 1. In order to limit the inter-symbol interference, each channel uses Frequency Division Duplexing (FDD) and is divided into several M-Quadrature Amplitude Modulation (M-QAM) sub-carriers, modulated at a lower bit rate (2400 symbols/s). Each channel of 25 kHz is sub-divided into 8 sub-carriers with a step of 2.7 kHz, so that the total symbol rate should be of 19,200 symbols/s.

By analysing the downlink logical channels [2] we notice that the frequency correction slot (SB) includes a sequence of 80 bytes with a fixed value. The simulations performed by us show that the transmission of this sequence generates a discrete spectral component in the power spectrum of the modulated signal. The frequency of the discrete spectral component is shifted by 2.25 kHz from the central carrier frequency (figure I).

The aim of the present paper was to analyse the energy detection of a TETRA signal and to that end we have used the radiometer technique, which we have implemented with a spectral analyser and a MATLAB software application. Probabilities of detection and of false alarm are investigated depending on measurement duration and measurement settings, in two representative cases, one on the central frequency of the TETRA channel and another on the discrete component frequency of the synchronization channel (SYNC).

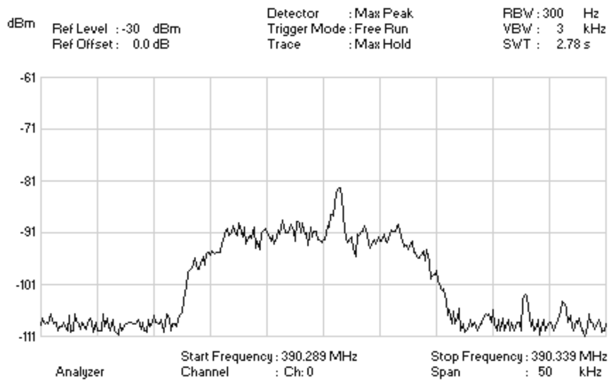

FIGURE I. POWER SPECTRUM FOR TETRA DURING SYNC BURST

II. METHOD AND MATERIALS

The detection of radio signals through energy measurement (radiometry) is one of the simplest techniques of signal detection, as it does not require additional information on the useful signal to be received. The radiometer parameters are: W - bandwidth and T - integration time. For digital radiometers, the duration T can be replaced with N - the number of samples. Five mathematical models describing the operation of the radiometer are compared and presented in [3]. These models use probability distributions for the energy output of the detection system, and the two forms it may take: presence of useful signal and absence of useful signal. The probabilities of false alarm and of detection are deduced from these distributions, depending on the Signal to Noise Ratio (SNR). If the number of samples used is high enough (>100), the output energy distribution can be approximated by a random variable having a Gaussian distribution, whereas the probabilities of false alarm (Pfa) and of detection (Pd) can be expressed with the following relations [4]:

$$P_d = Q[\frac{V_t - N_0 TW - E}{(N_0{}^2 TW + 2N_0 E)^{1/2}}],\quad P_{fa} = 1 - \Gamma(\frac{2V_t}{N_0}, \gamma) \quad (1)$$

where: $\Gamma(x) = \int_0^{\infty} y^{x-1} \exp(-y) dy$ - Gamma function, $\Gamma(x,a) = \frac{1}{\Gamma(a)} \int_0^{x} e^{-t} t^{a-1} dt$ - incomplete Gamma function, $Q(x) = \frac{1}{\sqrt{2\pi}} \int_x^{\infty} \exp(-\frac{u^2}{2}) du$ - Q function, N_0 – noise spectral

Digital Object Identifier 10.4316/AECE.2010.03015

density; T – measurement duration, W – radiometer bandwidth, E – signal energy and V_t – threshold value.

A spectral analyser (R&S FSH3) has been used for the practical implementation of the radiometer technique. We have compared the measured value with a threshold and have made a decision as to whether the signal is present or absent by importing and processing the results of measurements in the MATLAB environment (figure II). If we analyse the digital spectrum analyser [5, 6, 7] and the way it works, we will see that there is a correspondence between the parameters of the radiometer (W, T) and those of the spectrum analyser. Thus, the measurement bandwidth of the radiometer (W) corresponds to the resolution bandwidth (RBW) of the spectrum analyser. The relation between the measurement duration (T) and the sweep time (SWT) can be expressed as follows:

$$T = \frac{SWT}{N} \quad (2)$$

N represents the number of pixels used by the spectrum analyser for the graphical representation, and is 300 in the case of the FSH3 analyser.

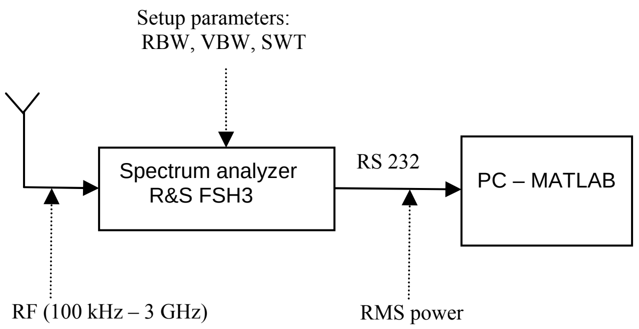

FIGURE II. BLOCK DIAGRAM OF MEASURING SYSTEM

By designing a software application to control the spectrum analyser, we have managed to automate the measurement process. The results of measurements have been processed in the MATLAB environment with the purpose of estimating the probability density function (PDF) of the power, measured for different settings (RBW and SWT).

We have used the Parzen window method [8]. If x_i represents the measured samples, the Parzen estimate will take the following form:

$$\hat{f}(x) = \frac{1}{nh(n)} \sum_{i=1}^{n} g\left(\frac{x - x_i}{h(n)}\right) \quad (3)$$

The kernel function g(y) and the smoothing coefficients h(n) are as follows:

$$g(y) = \frac{1}{\sqrt{2\pi}} \exp\left(\frac{-y^2}{2}\right), \quad h(n) = \frac{1}{\sqrt{n}} \quad (4)$$

The smoothing coefficient [8] determines the bias and the dispersion of the estimator. In our case, the value of the smoothing coefficient leads to an estimate with a reduced dispersion.

The estimator has been implemented in a MATLAB application. The estimation has been done in three stages: a first stage when the PDF of the spectrum analyser internal noise power was estimated, a second one when the PDF of TETRA downlink signal power was estimated and a third and last one, based on the previous two estimates, when the probabilities of detection and of false alarm were analysed.

Three hundred thousand (300,000) measurements have been performed for an estimation of the PDF. The measurement system settings' influence (RBW, SWT) upon the estimation accuracy has also been analysed both for the internal noise power and for the downlink TETRA signals' power.

III. RESULTS AND DISCUSSIONS

In order to measure the power of the internal noise we have replaced the antenna of the measurement system with an impedance of 50Ω. Figure III presents the results of the PDF estimation of the internal noise power for different resolution filters. The measurement time has been constant, with value of 0.2 ms. The graphical representation of power confirms the fact that the measured value is a variable with a Gaussian distribution. The average power as well as the standard deviations are presented in table I.

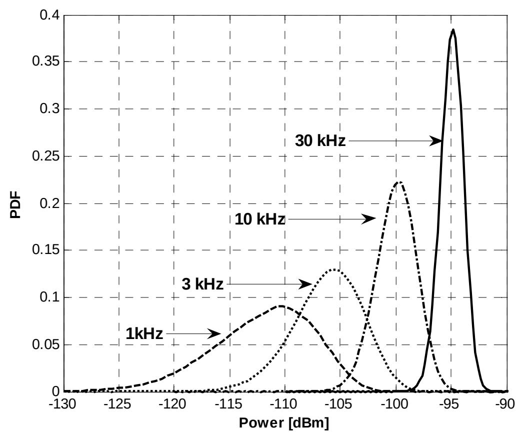

FIGURE III. PDF OF THE NOISE POWER FOR DIFFERENT RESOLUTION FILTERS

TABLE I. STATISTICAL VALUES OF NOISE POWER DEPENDING ON THE RESOLUTION FILTER

RBW	Average power	Standard deviation
1 kHz	-109.7669 dBm	3.8832 dB
3 kHz	-104.9477 dBm	2.5841 dB
10 kHz	-99.4731dBm	1.4575 dB
30 kHz	-94.7181 dBm	0.8366 dB

According to the results obtained, an increase in the resolution filter (RBW) entails a decrease in the PDF of the noise power. For a 10 times increase of the RBW the measured dispersion reduced with 1.4 dB. The average power increases along with the RBW. This increase in the measured value along with an increase in the RBW filter bandwidth can be quantitatively characterized by the *d* difference between the average measured powers for different values of the RBW:

$$d = 10\log_{10}\frac{RBW_1}{RBW_2} \text{[dB]} \quad (5)$$

If we compare the differences betwen the measured average powers (table II) and the theoretical values resulted from relation 5, we can see that the differences are smaller that 0.2 dB.

In order to study the effect of the measurement duration upon the power of the noise, we have repeated the previous measurements for RBW=1kHz and for different measurement durations (figure IV and table III). The results show that the average power is relatively constant regardless of the measurement duration. An increase in measurement duration will, however, entail a decrease in power dispersion.

In order to estimate the PDF of TETRA signals we have measured the channel power level of the broadcasting cell. The central measurement frequency of the spectrum analyser was set to be equal to the carrier frequency of the TETRA downlink channel.

TABLE II. STATISTICAL VALUES OF NOISE POWER ACCORDING TO MEASUREMENT DURATION

Measurement duration	**0.8 ms**	**1 ms**	**2 ms**	**3 ms**
Average power [dBm]	-109.7	-109.5	-109.5	-109.5
Standard deviation [dB]	3.11	2.84	2.0	1.7176

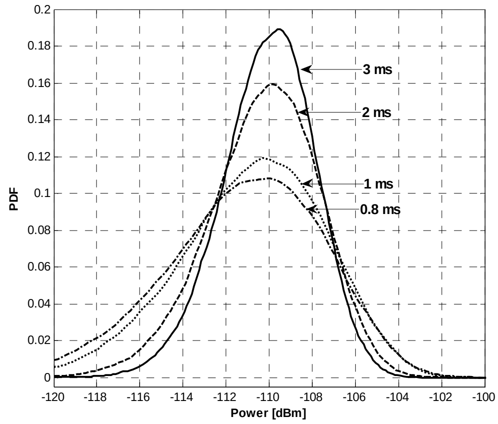

FIGURE IV. PDF OF NOISE POWER FOR DIFFERENT VALUES OF THE MEASUREMENT DURATION

In order to establish the effect of the resolution filter band upon the distribution of power, we have performed several measurements with different resolution filters. The measurement duration was constant and had a value of 0.4 ms. According to the results presented in figure V and table III, an increase in the filter resolution bandwidth from 1 kHz to 3 kHz led to an increase in the average power, from 97.9 dBm to 91.82 dBm. An increase in average power through the extension of filter bandwidth is accompanied by a reduction in power dispersion. By comparing the dispersion values, we notice that an increase in filter bandwidth from 1 kHz to 3 kHz, will lead to a decrease in power dispersion from 2.048 dB to 0.945 dB.

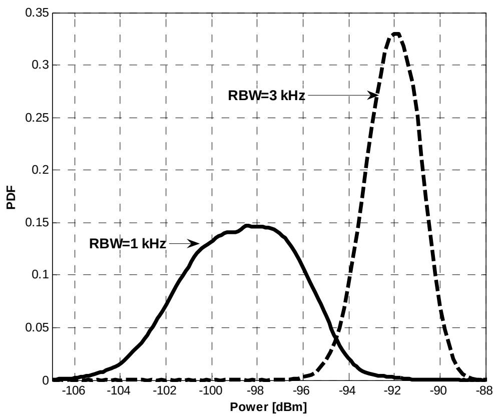

FIGURE V. PDF OF SIGNAL POWERS FOR DIFFERENT RESOLUTION FILTERS

In order to study the effect of measurement duration upon power distribution, we have measured the power for different measurement duration values and a constant RBW value. The results we have obtained (table IV and figure VI) show that an increase in measurement duration results in a decrease in power dispersion. The average power remains relatively constant. If the measurement duration is increased from 0.3 ms to 3 ms, the power dispersion decreases from 4.4 dB to 2.04 dB.

TABLE III. STATISTICAL VALUES OF POWER DEPENDING ON THE RBW

RBW	**1 kHz**	**3 kHz**
Average power [dBm]	-97.9	-91.82
Standard deviation [dB]	2.048	0.945

TABLE IV. STATISTICAL VALUES OF POWER DEPENDING ON THE MEASUREMENT DURATION

Measurement duration	**1 kHz**	**3 kHz**	**0.8 ms**	**3 ms**
Average power [dBm]	-98.91	-98.34	-98.34	-97.98
Standard deviation [dB]	4.4890	4.2593	3.5047	2.0489

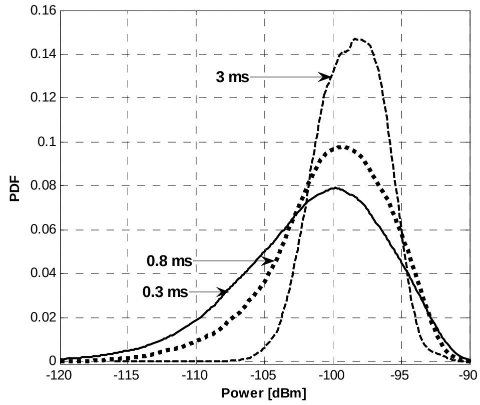

FIGURE VI. PDF OF SIGNAL POWER FOR DIFFERENT MEASURMENT DURATION VALUES

Figure I emphasizes the discrete spectral component corresponding to the synchronization burst. This spectral component lasts for 2.2 ms and is transmitted on the SYNC channel every 14.2 ms. By starting from the assumption that the power of the discrete spectral component corresponding to the frequency correction sequence is higher as compared to the other spectral components, we have measured the power on the synchronization frequency. We have studied the effects of the filter resolution bandwidth and of the measurement duration upon the power PDF. The effects of the measurement duration are presented in figure VII. Measurements have been carried out with a resolution filter of 1kHz.

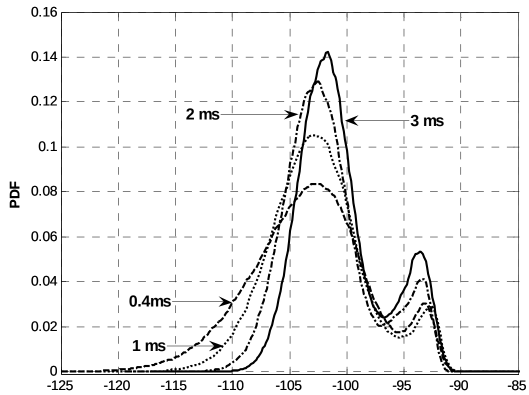

FIGURE VII. PDF OF THE SYNC COMPONENT POWER FOR SEVERAL VALUES OF MEASUREMENT DURATION

If we compare the PDF shapes we can see that when the measurement is done with RBW filters and a bandwidth of 1 kHz and 3 kHz, the periodical bursts of power corresponding to the synchronization channel (SCH) are emphasized. Probability distribution reaches a local maximum at the average power value of the discrete component. When the measurement is done with a filter of 10 kHz, the discrete spectral component can no longer be emphasized due to the low selectivity. The effect of increasing the measurement duration is the same as in the case we have already discussed, i.e. power dispersion decreases whereas the average value of the power remains relatively constant. We have calculated the probabilities of detection and of false alarm for different values of the spectrum analyser's parameters (RBW, SWT) as well as for different SNR values. The SNR has been estimated based on the ratio between the average value of the useful signal and the average power of the noise. The value of the SNR was corrected using an error coefficient due to $SNR_{measured}$ [6].

The probabilities of detection and of false alarm have been calculated based on the estimate probability density function, for different values of the RBW and of the measurement duration, their graphical representation being presented in figures VIII and IX.

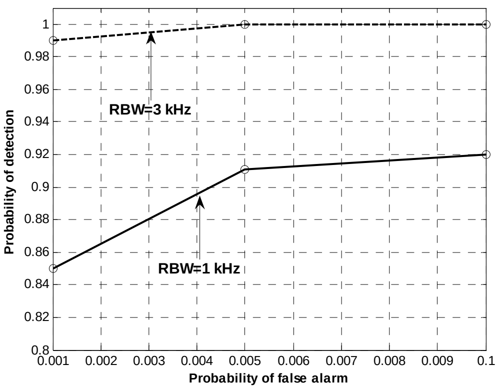

FIGURE VIII. PROBABILITY OF DETECTION VS. PROBABILITY OF FALSE ALARM FOR DIFFERENT RBW FILTERS

It can be seen that the higher the accepted probability of false alarm, the bigger the value of detection probability. If the measurement duration values are about 3 ms and SNR=11.2 dB, the detection probability is almost 1 for all the 3 values of the imposed probability of false alarm.

By analysing the case when measurements are performed on the SYNC channel, we can see that a filter with a reduced occupied band entails an increase in $SNR_{measured}$ with values ranging from 1 dB to 7 dB, as compared to the power measurements on the central frequency. The highest increase in SNR is obtained for reduced RBW values (1kHz). For RBW values higher than 3 kHz, SNR decreases up to the point where, for RBW=10 kHz its value is 0. An increase in measurement duration will also lead to an increase in SNR. If the measurement duration is changed from 0.4 ms to 3 ms, SNR will be increased by 3 dB, for a filter with RBW=1 kHz. In the case of a TETRA signal with SNR=20 dB and a 0.001 imposed probability of false alarm, this increase in $SNR_{measured}$ is translated into an increase in detection probability from 0.88 to 0.93, when the measurement is performed on the SYNC channel. An increase in RBW, from 1 kHz to 3 kHz, will reduce the difference between the average powers measured on the central channel and the SYNC channels, from 4 dB to 1 dB. This effect can be explained by the fact that, while the selectivity of the resolution filter decreases, the bandwidth increases.

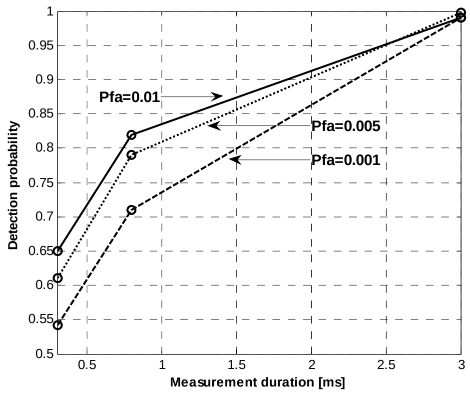

FIGURE IX. PROBABILITY OF DETECTION VS. DURATION

IV. CONCLUSION

Detection and false alarm probabilities assessment highlighted the way by which the measurement system's parameters could be optimised in order to maximise the detection probability, provided that an acceptable value is set for the false alarm probability. Based on the results, we can draw the following conclusions:

- an increase in measurement duration will result in an increase in detection probability;
- an increase in filter resolution bandwidth will result in an increase in detection probability, as long as the resolution filter band is narrower than the band of the measured signal;
- the optimum value of the resolution filter is equal to the value of the occupied band of the measured signal;
- the TETRA signals detection probability increases when the power is measured on the frequency of the discrete spectral component corresponding to the SYNC channel;
- if power is measured on the synchronization channel, it is recommended that the filter band should be as narrow as possible (high selectivity) in order to maximize the detection probability.

ACKNOWLEDGMENT

The work was supported by a grant financed by the Romanian Ministry of Education and Research, through Contract no. 367/2007 from CNCSIS - "Idei" Programme.

REFERENCES

[1] *** ETSI EN 300 392-2 V3.2.1, 2007, Terestrial Trunked Radio (TETRA); Air Interface, 2007.
[2] Stavroulakis P., Terrestrial Trunked Radio – TETRA, Springer, Berlin, 2007.
[3] Poison R., Target Acquisition in Communication Electronic Warfare Systems, Artech House, Boston, 2004.
[4] Torrieri D., Principles of spread spectrum systems, Springer, 2005.
[5] Rauscher C., Fundamentals of Spectrum Analysis, München, Germany, 2001.
[6] *** Spectrum Analysis Basics, Agilent, Aplication Note 150.
[7] *** Spectrum Analyzer-Measurements and Noise, Agilent, Aplication Note1303.
[8] Martinez W., Martinez A., Computational Statistics Handbook with MATLAB, Chapman & Hall, 2002.